UC Santa Barbara

Title

Overlapping Spreading Center System at 12054, N on the East Pacific Rise, Marine Geographical Researches 9

Permalink

Authors

Antrim, Lisa
Sempere, Jean-Christophe
Macdonald, Ken C
et al.

Publication Date

2023-12-10

Peer reviewed

Fine Scale Study of a Small Overlapping Spreading Center System at 12°54′ N on the East Pacific Rise

LISA ANTRIM[1], JEAN-CHRISTOPHE SEMPERE[2], KEN C. MACDONALD

Department of Geological Sciences and Marine Science Institute, University of California, Santa Barbara, CA 93106, U.S.A.

and

F. N. SPIESS

Marine Physical Laboratory, Scripps Institution of Oceanography, University of California, San Diego, La Jolla, CA 92093, U.S.A.

Abstract. Overlapping spreading centers (OSCs) are a type of ridge axis discontinuity found along intermediate and fast spreading centers. The ridges at these locations overlap and curve towards each other, and are separated by an elongate overlap basin. A high resolution Deep-Tow survey was conducted over the 12°54′ N OSC (offset ∼1.6 km) on the East Pacific Rise in order to study the structure of a small OSC on a fine scale. A detailed tectonic study and Deep-Tow 3-D magnetic inversion were performed on the data. Towards the tips of both limbs, the apparent age of lava flows increases, the density of exposed faults and fissures increases, and the axial graben loses definition and disappears. No active hydrothermal vents were detected in the area. These observations suggest that the magmatic budget steadily decreases along axis approaching an OSC, even where the offset is small. In contrast with OSCs which have a large offset (>5 km), the 3-D magnetic inversion solution for this OSC produced no evidence for highly magnetized areas near the tip of either spreading center.

1. Introduction

Recent high resolution studies on intermediate and fast spreading centers (>4–6 cm yr^{-1} full rate) have led to the recognition of families of non-transform ridge axis discontinuities whose offsets are small (<0.3 million years) in comparison with offsets observed at transform faults and large propagating rifts (Macdonald *et al.*, 1984, 1986; Lonsdale, 1983; Langmuir *et al.*, 1986; Batiza and Margolis, 1986). These discontinuities include smaller propagating rifts, overlapping spreading centers (OSCs), saddle points, deviations

from axial linearity (DevALs), and small non-overlapping offsets (SNOOs). In view of the tiny age contrast at these ridge axis discontinuities, the thermal edge effects used to explain the anomalous depths and crustal structure observed near transform faults (e.g., Fox and Gallo, 1984) do not adequately explain the depth, petrologic or magmatic anomalies at these small offsets. Instead these discontinuities appear to be related to the thermal and magmatic budget associated with melting events in the upper mantle beneath the ridge (Macdonald *et al.*, 1984; Schouten *et al.*, 1987).

At overlapping spreading centers, the rise axes overlap in an *en échelon* sense, curve towards each other, and are separated by an elongate overlap basin (Macdonald and Fox, 1983; Macdonald *et al.*, 1984; Lonsdale, 1983, 1985). The frequency of occurrence of these features along the East Pacific Rise (EPR) suggests that they are a significant aspect of crustal accretion processes at intermediate and fast spreading rates (Figure 1). A detailed comprehensive investigation of a large OSC (offset ∼8 km) at 9°03′ N on the EPR has been completed (Sempere *et al.*, 1984; Sempere and Macdonald, 1986b), but OSCs have remained relatively unstudied on a fine scale. This project, a Deep-Tow survey over the 12°54′ N OSC conducted in January of 1985 aboard the R/V Melville, provides the most comprehensive high resolution mapping of a small OSC to date. The variety of data collected, including side-looking sonar images, and high resolution bathymetry, photographs, water temperature, and near-bottom magnetic field measurements as well as detailed rock sampling, allows
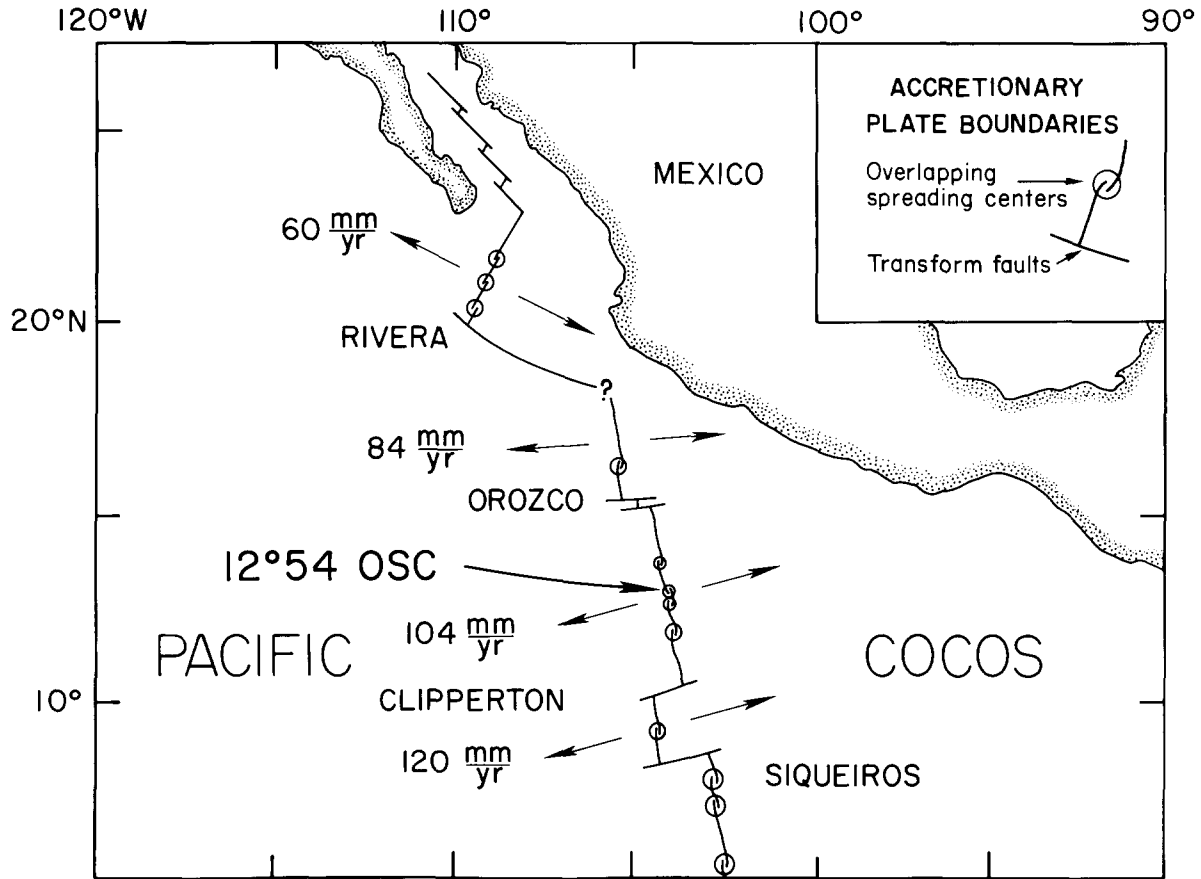
Fig. 1. Overlapping spreading centers have been mapped between 21°S and 22°N on the East Pacific Rise (Macdonald and Fox, 1983; Macdonald et al., 1984; Lonsdale, 1983; 1985). The small (offset ~1.6 km) 12°54′ N OSC is the focus of this high resolution Deep-Tow survey.

for analysis of the feature from several different perspectives. Three other OSCs were investigated during this same cruise: near 9° N (Sempere and Macdonald, 1986b), 5°30′ N, and 4° N (Lonsdale and Spiess, unpublished data); and in each case, a detailed sampling program was also conducted (Natland et al., 1986).

At the latitude of the 12°54′ N OSC, the EPR has an opening rate of 11 cm yr^{-1} (Klitgord and Mammerickx, 1982). The offset was first mapped by Macdonald and Fox (1983) with the Sea Beam multibeam echo-sounding system. The feature coincides with a local low in the axial depth profile, as do all other OSCs and many other ridge axis discontinuities. It is bordered on the south by a region with active hydrothermal vent fields (Hekinian et al., 1982; Francheteau and Ballard, 1983). Dives with the French submersible CYANA provided descriptions of the tectonic and geologic settings for the nearby hydrothermal activity (Ballard et al., 1984; Choukroune et al., 1984) as well as observations over the OSC, including petrologic compositions of several samples from the area (Hekinian et al., 1985). A combined SeaMARC

I and Sea Beam cruise along the EPR included tracks over and off axis from the 12°54′ N OSC (Crane, 1987). Finally, a seismic refraction survey has been conducted near the 12°54′ N OSC by McClain et al. (1985), and Detrick et al. (1987) have completed a multi-channel seismic reflection survey directly over the feature.

2. The Survey

The survey was conducted using the Deep-Tow instrument package of the Marine Physical Laboratory (Scripps Institution of Oceanography) (Spiess and Tyce, 1973; Spiess and Lonsdale, 1982). The instrumentation includes side-looking sonars, a narrow beam down-looking sonar, a 4 kHz seismic profiler, a proton precession magnetometer, three 35 mm cameras, a snapshot television, and a standard Neil Brown conductivity-temperature-depth (CTD) instrument. The vehicle is towed 10–150 m above the seafloor. Track spacing in the survey averaged only 400 m, providing very dense coverage. Accurate positioning

was accomplished through a combination of satellite and transponder navigation.

Detailed bathymetry is obtained with the Deep-Tow system through a combination of pressure sensor readings from the CTD indicator and sonar recordings from a 125 kHz downlooking sonar which has a beam width of only 2°. This provides a high resolution profile of the seafloor, delineating scarp heights and bathymetric variations accurate within less than a meter. Twin side-looking sonars have beam widths which are broad in the vertical sense (60°) but narrow horizontally (3/4°), and are operated at 110 kHz. The records are images of energy reflected from features up to 750 m on either side of the vehicle and include detailed information about location, orientation, and size of faults, fissures, and flow fronts. While the sonar systems supply the bulk of the data for structural analyses, the photographic data provide supportive detail as well as information about age relationships, sediment cover, volcanic flow forms, and hydrothermal activity. A proton precession magnetometer measured the total magnetic field every 29 s (approximately every 25 m along track). The portion of the survey used in the three dimensional magnetic inversion was conducted at a constant depth of 2550 m in order to avoid the necessity for upward continuation of the data in the calculations.

3. Summary of Tectonic Observations

The overlapping spreading centers at 12°54′ N consist of two ridges that curve slightly away from each other just before they overlap and curve towards each other (Figure 2). Their left-stepping offset is 1.6 km, measured perpendicular to the limbs at their point of maximum separation. The axes are separated by an elongate basin 80 m in depth, and overlap by 5.0 km. The two axes are of a similar height, and towards the tip of either limb the axial graben becomes less prominent until it disappears altogether (Figures 3, 4).

Extensive faulting and fissuring occur on the rise axes, with a slight increase in density towards the tips up to the last kilometer, where the density of faulting and fissuring decreases again (Figure 5). The faults range in throw from undetectably small to 30 m, with an average throw of 8.5 m. The strike of the faults and fissures on the axes generally follows that of the ridge axes, with an average orientation of 345°. Faults striking at a high angle to the tips which would indicate a transform fault type of offset are not observed.

Slightly off-axis the majority of faults and fissures follow an orientation parallel to the curving spreading centers. Presumably faults and fissures which are within approximately 5 km of the axis are under the influence of the same stress field which produces the curving of the spreading axes (Sempere and Macdonald, 1986a). The lateral spacing of near-axis faults is considerably greater than on-axis in most places (Figure 5) suggesting that many near-axis faults and fissures have been buried by lava flows.

The basin separating the two axes is nearly devoid of tectonic lineations, and is characterized almost entirely by volcanic constructional features. It is bounded by volcanic slopes with no evidence for normal faulting or collapse to account for the 80 m deep basin.

A volcano located 1.5 km south of the tip of the western limb is 80 m high and 1 km wide. It shows no fault structures other than an elongated crater on its summit. A 40 m high ridge parallel to and 0.5 km east of the eastern limb of the OSC has a width approximately half that of the OSC ridges. It appears to be volcanic in origin and is highly faulted and fissured. The density of faulting and fissuring at the northern end of the ridge is comparable to that of the OSC axes, but decreases towards the south. The average strike of the lineations is 345°, parallel to that of the ridge. It may represent a relict or decapitated ridge tip from an earlier stage in the development of this OSC.

Relative ages of lava flows were determined through analysis of Deep-Tow photographs for the amount of sediment cover and for the degree of vitreous luster of the flow surfaces (Figure 6). The youngest lavas occur on the western spreading center at the northern end of the zone of overlap (Figures 6b, 7). Closer to the tip, the sediment cover increases. A pattern of increasing age towards the tip is very apparent from extensive photographic coverage on the eastern spreading ridge (Figure 7). The off-axis ages as well as those of the basin and southern volcano are older than the relatively young flows on the ridges. The flows in the area are predominantly pillow basalts, but sheet flows occur between the ridges at the southern end of the overlap zone and just west of the southern volcano. No active hydrothermal vents were detected, but some hydrothermal staining and sparse biological activity can be observed on both limbs in the vicinity of very recent volcanism. The nearest active vents are located at 12°51′ N in the French survey area, approximately 2 km south of the southern end of the OSC (Choukroune et al., 1984).
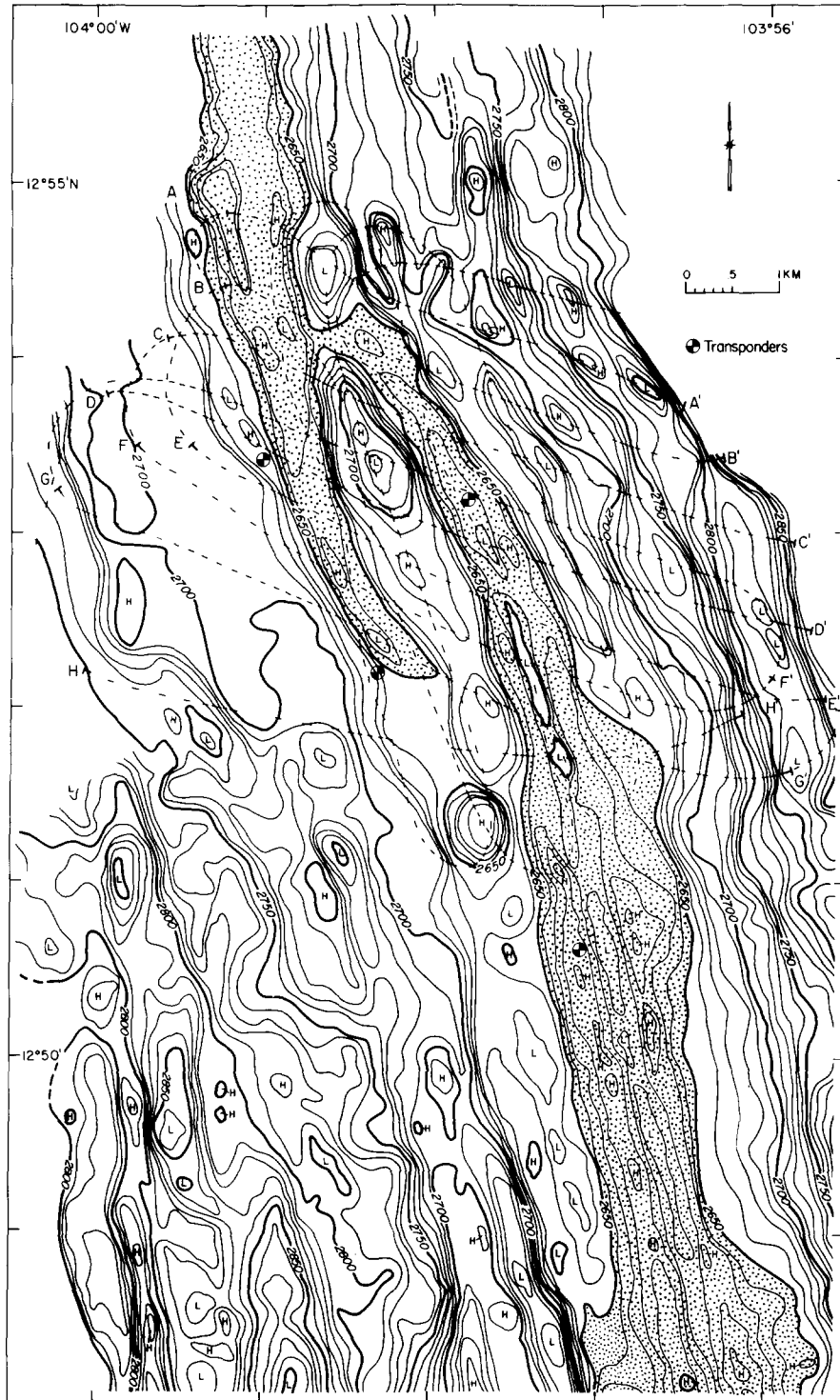
Fig. 2. Bathymetric map of the 12°54' N OSC (contour interval = 10 m) generated by combining high resolution Deep-Tow bathymetry with existing Seabeam maps (Francheteau and Ballard, 1983; Macdonald and Fox, 1983; Hekinian et al., 1985). The Deep-Tow tracks for the survey are shown with contour crossing ticks and dashed lines. Circles show locations of navigational transponders and letters show the end points of the Deep-Tow profiles in Figure 3. The rise axes at the OSC overlap for 4.9 km, are offset 1.6 km, and are separated by an 80 m deep basin.
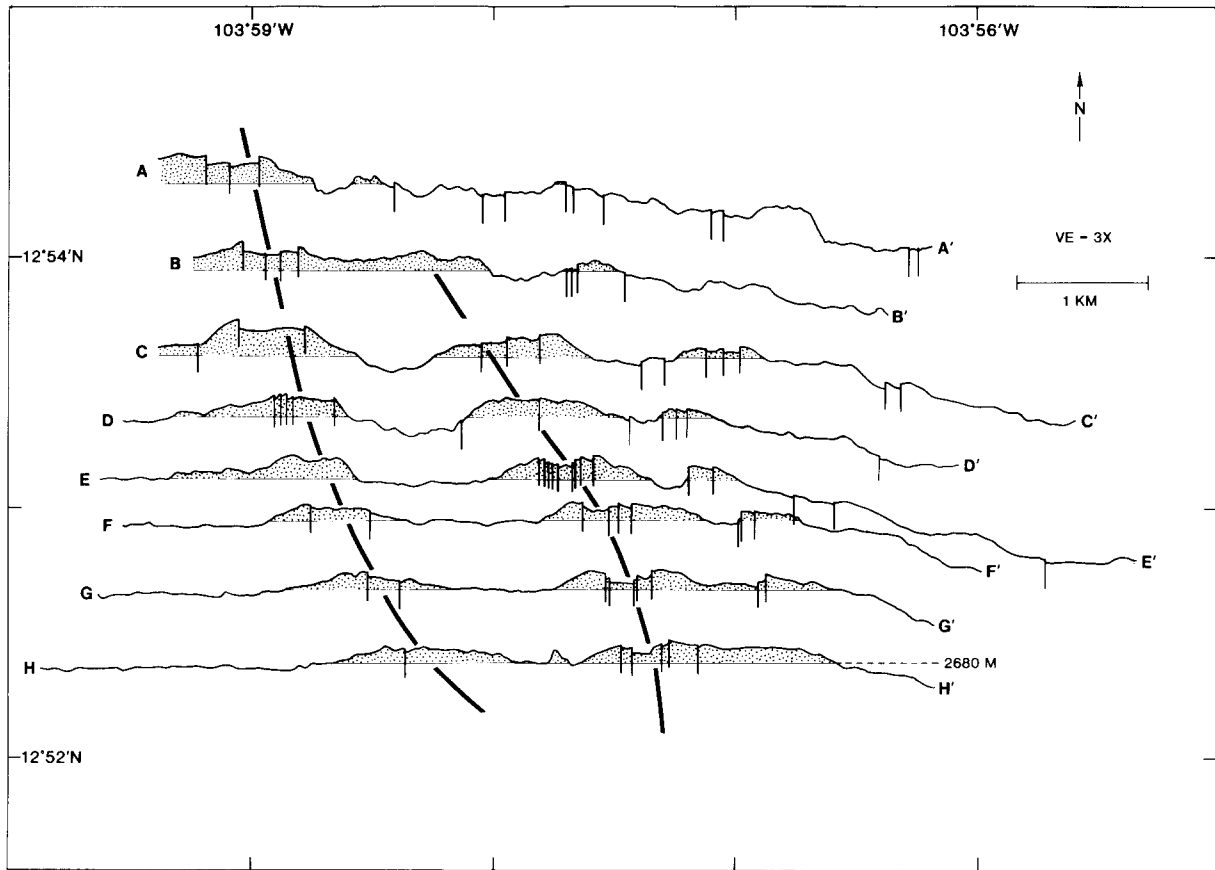
Fig. 3. Detailed bathymetric profiles from narrow beam down-looking sonar projected east-west. (Horizontal datum line is 2680 m.) Both these data and side-scan sonar data were used to interpret dip-slip faults shown by vertical lines. Dark lines indicate the OSC axes. The axial graben loses definition and disappears towards the tips of both limbs at about the same place where a seismic reflector interpreted to be the roof of a magma chamber disappears (Detrick *et al.*, 1987).

4. Magnetic Studies

Bathymetric roughness can contribute significantly to the measured magnetic field anomaly (Miller, 1977), so in order to assess the magnitude of bathymetric influence on the data in the survey area, a forward model of the magnetic field due to a uniformly magnetized, constant thickness layer following the bottom topography was calculated. The Fourier method used in generating the model was devised by Parker (1972). A uniformly magnetized (20 amp m^{-1}), 1 km thick layer coinciding with the bathymetry at the 12°54′ N OSC was input as a source for the calculations. The remanent magnetization vector was determined for the location assuming an axially geocentric dipole. The resulting forward model, a theoretical magnetic anomaly due to the described source, is shown in Figure 8 along with the observed magnetic anomaly. Significant differences are apparent between the two,

indicating that, although bathymetric effects can be important, the variation observed in the data cannot be attributed to bathymetry alone.

A 3-D inversion was performed to remove the topographic and ridge orientation effects from the data. The Fourier method used was originally formulated for the two dimensional problem by Parker and Huestis (1974), and has been extended to three dimensional applications by Macdonald *et al.* (1980). The inversion uses an iterative procedure to solve for the source magnetization in the presence of the bathymetry. As with the forward model, a uniformly thick source layer following the bathymetry with a constant magnetization in the vertical direction was assumed. The observed Deep-Tow magnetic anomaly and bathymetry were gridded using the algorithm of Kennedy *et al.*, (1984) which applies the concept of lattice tuning (Tobler, 1979) by iterative use of the biharmonic finite difference operator to insure both
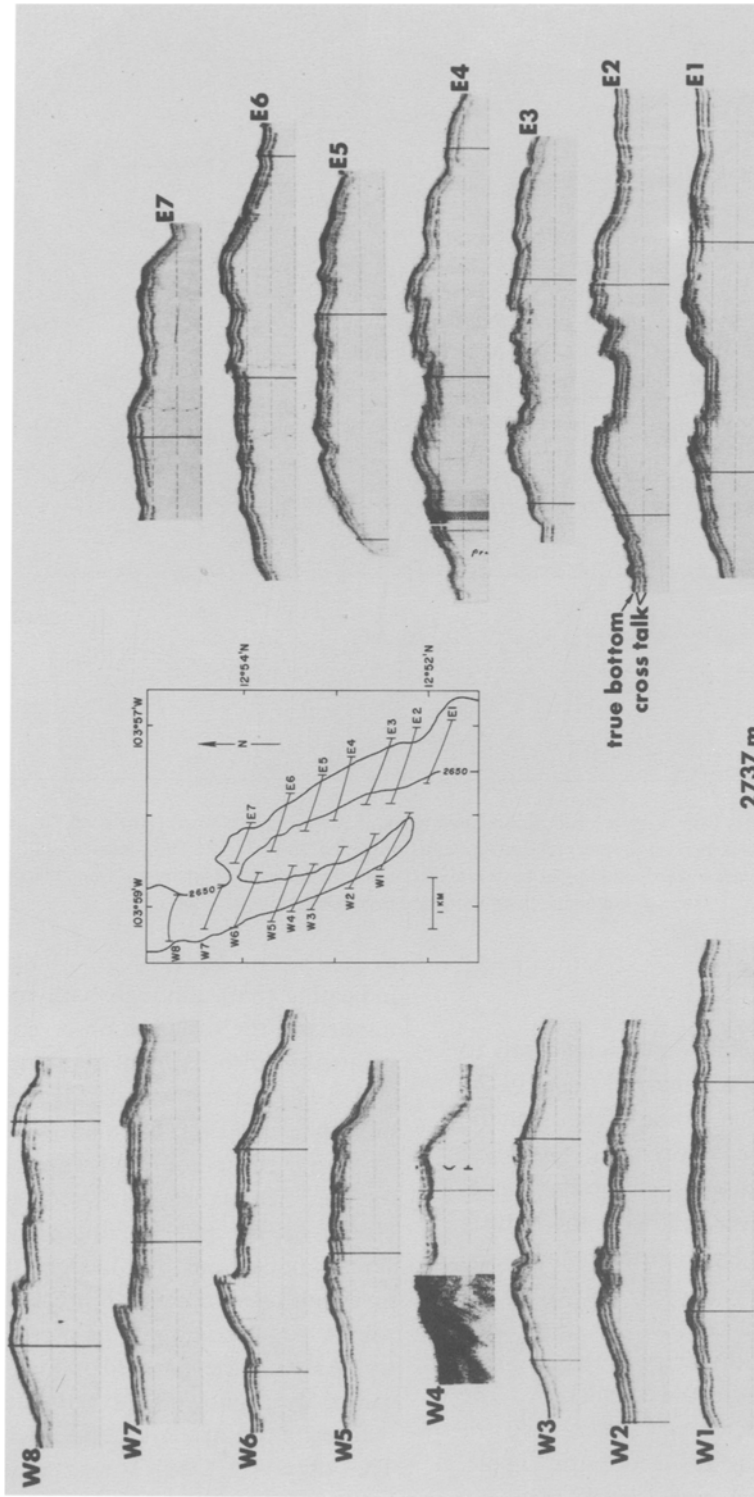
Fig. 4. Raw records of narrow beam down-looking sonar trace added to pressure signal showing axial crossings. True bottom corresponds to the top trace. The axial graben is not resolvable for the western limb on traces W1–W4, and on traces E5–E7 for the eastern limb. Second and third traces are cross talk, generated by signals from other transducers (side-looking sonars and forward-looking sonar).
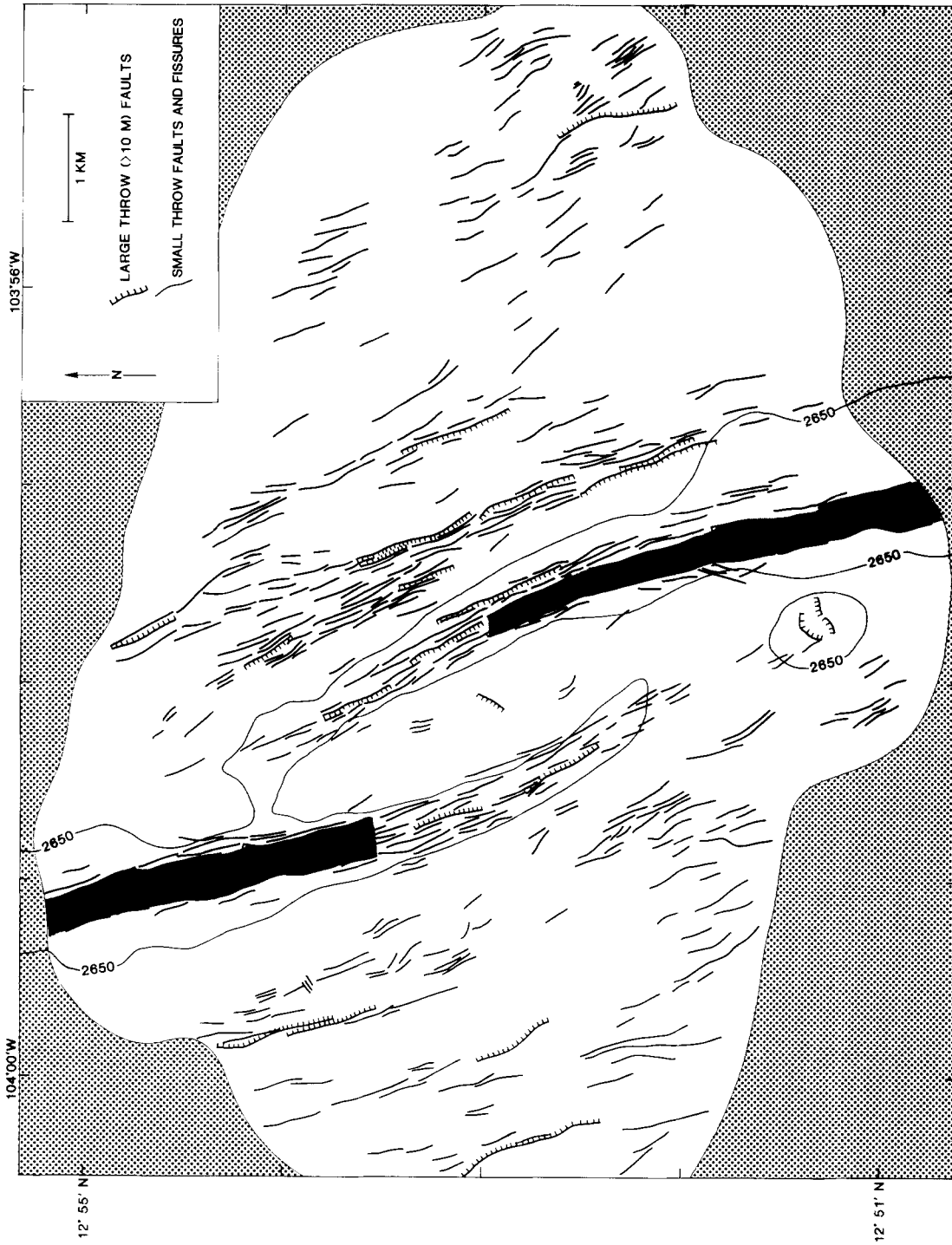
Fig. 5. A detailed tectonic map of the 12°54′ N OSC showing faults and fissures mapped by the side-looking and down-looking sonars. Fault throws were determined from narrow beam down-looking sonar records. Side-scan sonar coverage is continuous or overlapping except in the coarsely stippled zones. The axes, outlined by the 2650 m contour, are highly faulted and fissured, with fault density increasing towards the tips. The basin is nearly devoid of tectonic lineations. The axial graben, *highlighted by light shading*, loses definition and disappears towards the ends of both axes. A highly faulted ridge just east of the eastern spreading center may be an abandoned ridge tip (see text).
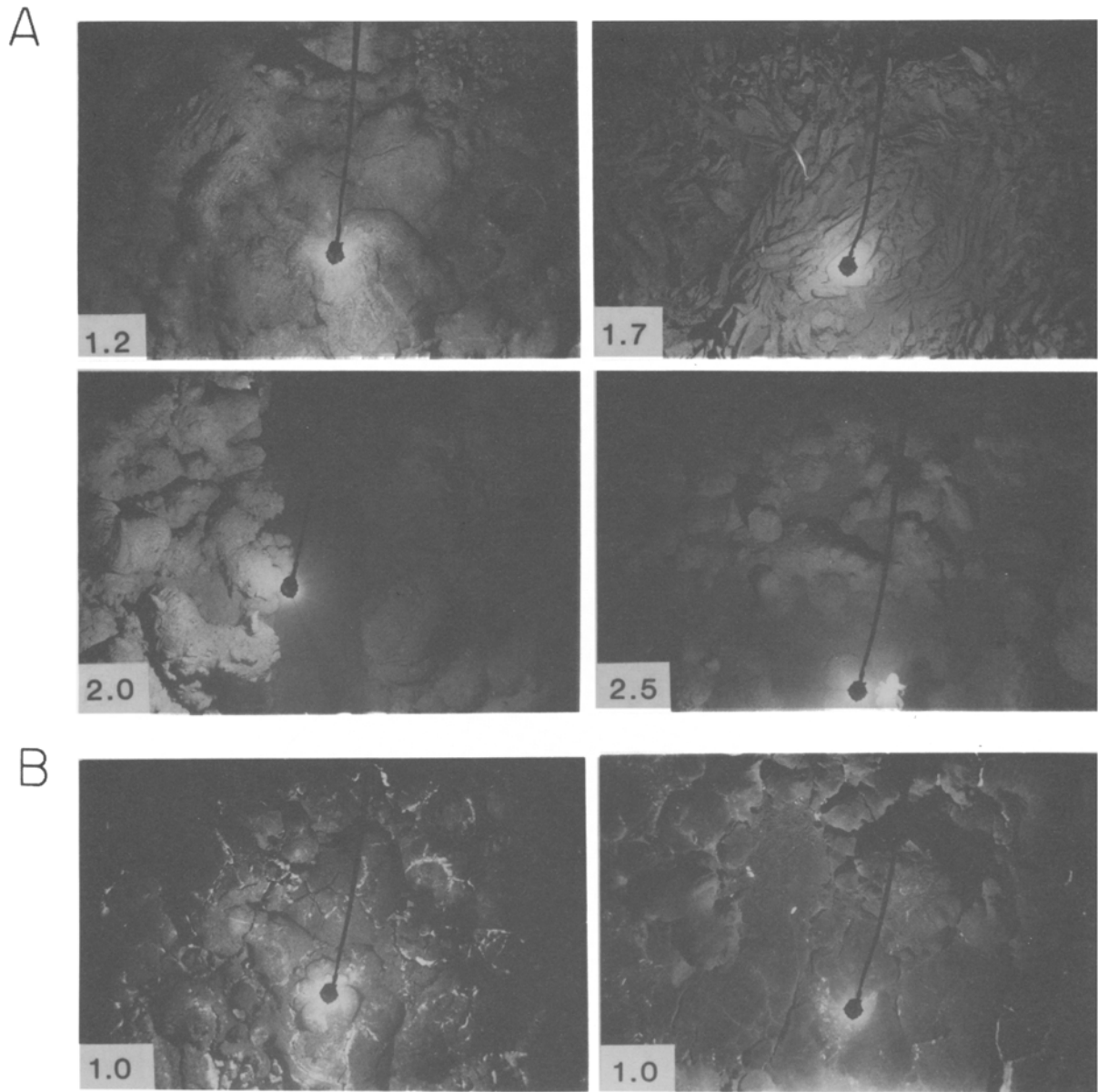
Fig. 6. (a) Bottom photographs taken from the Deep-Tow vehicle near 12°54' N representing the relative age scale used in estimating the age of lava flows. The scale is based on sediment cover and vitreous luster, where 1 is the youngest and 4 is the oldest (total sediment cover), similar to the scheme of Ballard *et al.* (1979). The photos are approximately 5 m across. (Upper left) flattened and lobate pillows showing local collapse; (upper right) sheet flows; (lower left) fissure; (lower right) older pillows, hooded octopus near strobe. (b) Very young flows observed on the western spreading limb near the northern end of the zone of overlap (see Figure 7). Bright yellow-orange (as determined from color photos) hydrothermal staining is visible around the edges of the cracks in the first photo. The staining appears as a white rind bordering the cracks in the pillows in these black and white photos.

smoothness of the gridded values and a good fit to the original data. Input for the inversion consisted of the two gridded data sets (with grid spacing of 250 m), the source layer thickness (1 km), and the ambient field direction.

As is always the case with potential field problems the solution is nonunique. There exists a magnetiza-tion for a given bathymetry which produces no exter-nal field called the annihilator, and any amount of it can be added to the solution without affecting the observed field. We normally add or subtract a certain amount of the annihilator magnetization to make positive and negative magnetizations across a reversal boundary approximately equal. Since no reversal
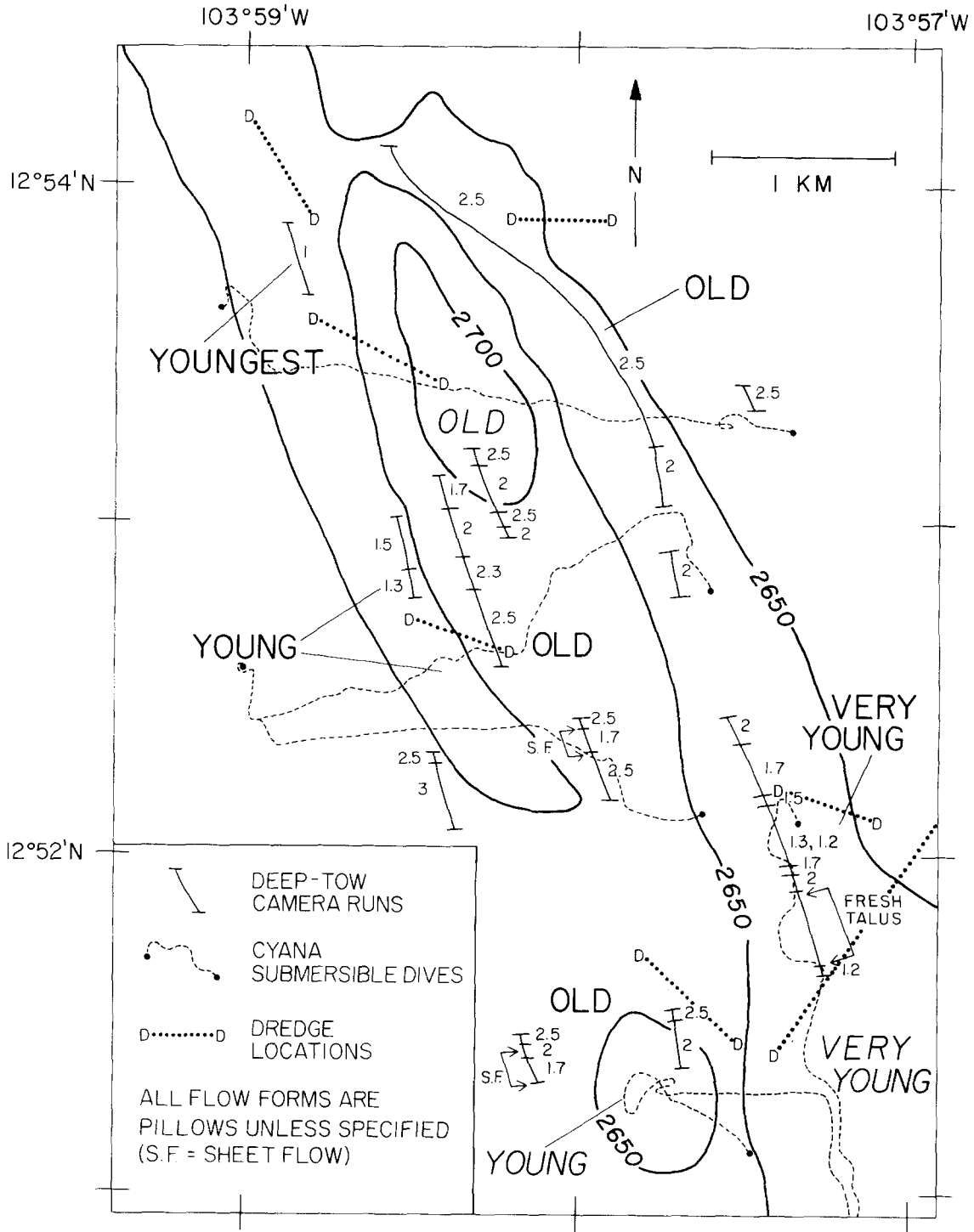
Fig. 7. Relative ages of lava flows determined from Deep-Tow camera runs (normal type and all numbers) and CYANA submersible data (slant type, after Hekinian et al., 1985). Locations of dredge hauls taken during this study as indicated. Very young flows are observed on both axes, with age increasing towards the tips. Flows are mostly pillows, with only two areas exhibiting sheet flows (S.F.). Large labels e.g. 'Young' indicate general pattern of relative ages in the area.
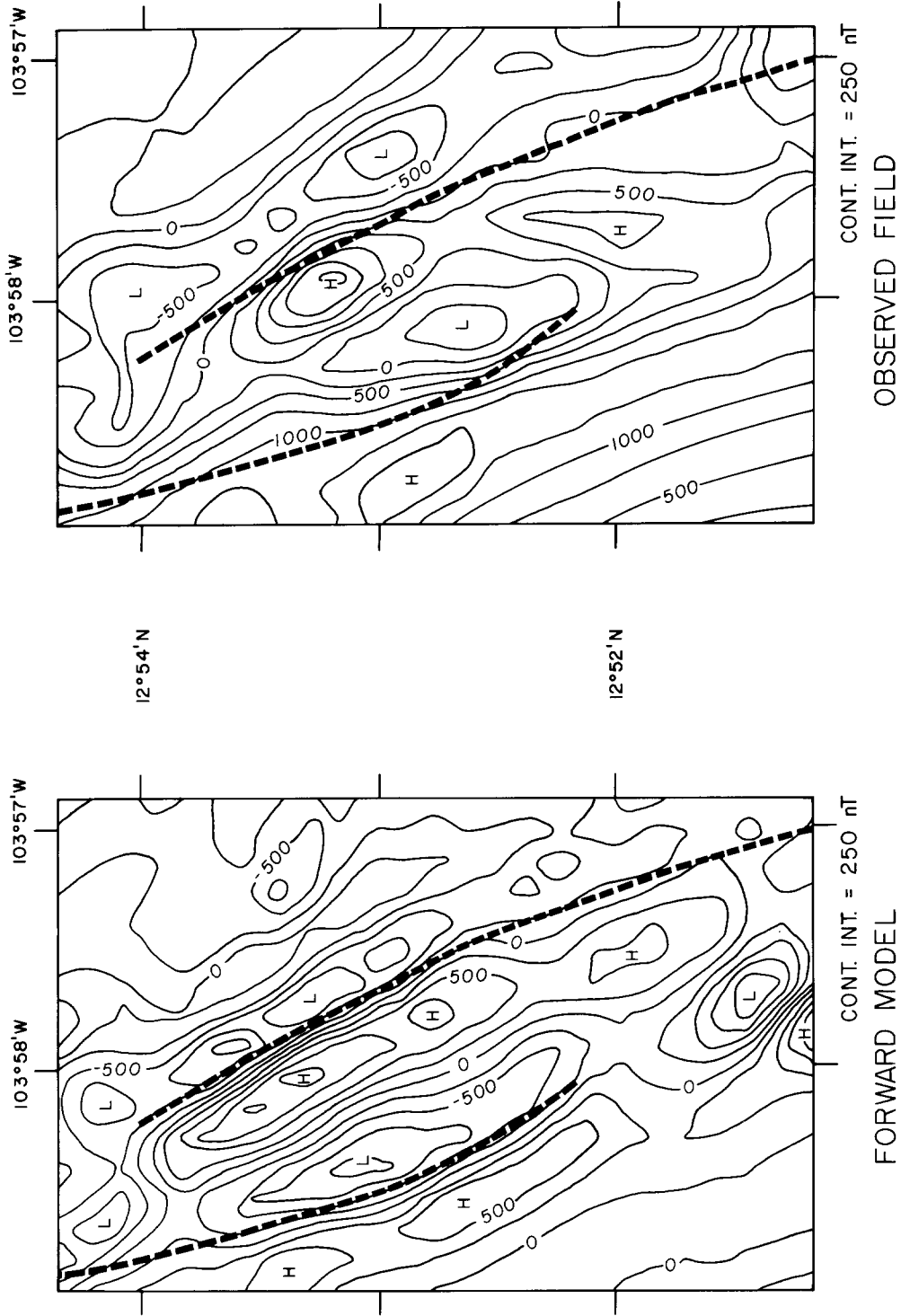
Fig. 8. (left) The magnetic field over the 12°54′ N OSC (axes shown with heavy dashed lines) obtained from forward modeling. The source is assumed to have a constant thickness (1 km) following Deep-Tow bathymetry and a constant magnetization (20 amp m^{-1}) following an axially geocentric dipole. The grid spacing is 250 m. (Right) The observed magnetic field over the 12°54′ N OSC (IGRF has been removed). There is disagreement with the forward model in both amplitude and distribution of anomalies, suggesting that non-topographic effects may be influencing the signal.

boundaries were crossed in this survey, we inverted several nearby long profiles which did cross several reversals. We determined an average axial magnetization of 15 amp m^{-1} for this area and added enough annihilator to our 3-D solution to produce a 15 amp m^{-1} background magnetization. Significantly different amounts of annihilator were also considered but did not change the shape or distribution of the solution, only its absolute level.

Three local maxima occur in the solution to the inversion (Figure 9), each with a maximum intensity of approximately 25 amp m^{-1}. Two correspond with the regions of most recent volcanism (as determined from the photographic data) on either limb of the overlapping system, while a third occurs over the southern volcano. The amplitude for the basin is comparable to that just off axis from the OSC. A minimum of 10–11 amp m^{-1} in the magnetization solution occurs in the overlap basin. (The positions and relative amplitudes of the maxima and minima mentioned do not change with differing amounts of annihilator).

5. Discussion

The structural and volcanic variations observed approaching the tips of either limb of the OSC are suggestive of tectonic processes which vary along strike. The concept of a longitudinal flow of melt was introduced by Vogt and Johnson (1975) and subsequently employed in numerous hypotheses to explain along strike variation on mid-ocean ridges (Vogt, 1976; Crane, 1979; van Andel and Ballard, 1979; Francheteau and Ballard, 1983; Macdonald et al., 1984; Crane, 1985). We have proposed that basaltic melt is episodically emplaced at discrete locations along the EPR resulting in swelling of the axial magma chamber, and a migration of melt along the strike of the ridge away from the loci of emplacement (Macdonald et al., 1984, 1986). Inflation of the axial magma chamber stretches the overlying brittle carapace, causing it to fracture. The cracks preferentially align perpendicular to the direction of least compressive stress, roughly corresponding to the strike of the ridge. We have suggested that OSCs form between locations of melt emplacement, and result from the migration of two magmatic pulses towards each other following fracture systems and conduits which are not perfectly aligned. If formed from such a process, OSCs should correspond to magmatically 'starved'

regions. Evidence for a starved region is present in various forms at the 12°54′ N OSC. It is situated at a low along the axial depth profile. No active hydrothermal vents were detected within the survey area (in contrast to the axial high just south of the region which contains numerous active fields (Hekinian et al., 1982; Ballard et al., 1984; Choukroune et al., 1984)) and the lavas appear to be older in a time averaged sense than lavas at nearby shallow portions of the ridge axis. In addition, the axial summit graben diminishes and disappears on both spreading centers in the overlap region which may be indicative of a reduced magmatic budget (discussed below).

Detrick et al. (1987) have recently suggested that the axial magma chamber is discontinuous across the OSC at 12°54′ N based on multi-channel seismic reflection data. In fact, the reflector associated with the hypothesized magma chambers disappears near the same place where the summit graben disappears on both the east and west spreading centers. This correlation exists elsewhere along the spreading center, suggesting that the presence or absence of an axial summit graben is significant. Where the rise axis is deep and has a small cross-sectional area, an axial summit graben and a 'magma chamber' reflector are absent suggesting a local low in the axial magmatic budget (Macdonald and Fox, submitted).

Ballard et al. (1979) and Francheteau and Ballard (1983) have proposed that an increase in the eruption of pillow flows relative to sheet flows occurs with increasing distance from the source in response to a decrease in supply and an increase in channeling of the magma. While there is considerable controversy over this matter, the high pillow to sheet flow ratio observed at the 12°54′ N could be another indication of a reduced magma supply. The observed flow forms in the vicinity of the 12°54′ N OSC were predominantly pillow basalts, with the exception of two sites displaying sheet flows. Both of these were located to the southern end of the region, which borders the area of robust hydrothermal activity to the south characterized by copious ponded lavas (Ballard et al., 1984).

The lack of hydrothermal activity, the high pillow to sheet flow ratio, and the location of the 12°54′ N OSC at a low along the axial depth profile all suggest a low magmatic budget. The age relationships from the area and the disappearance of the axial graben also suggest a diminishing supply towards the OSC (Macdonald and Fox, submitted). Both SeaMARC I
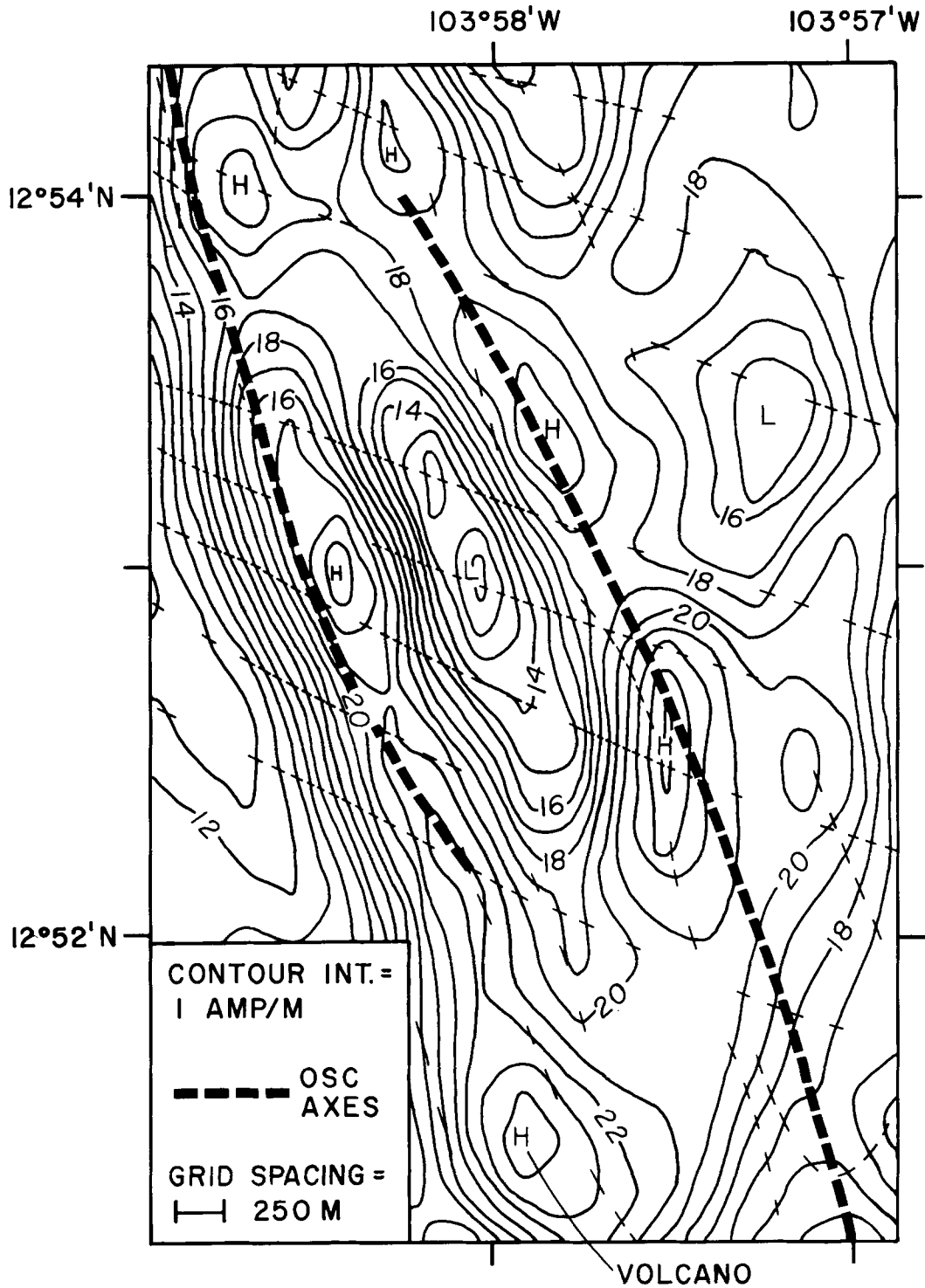
Fig. 9. Magnetization distribution at the 12°54' N OSC. Survey tracks used are shown as contour crossing ticks. Positive magnetizations of comparable magnitude (~25 amp m⁻¹) are associated with the two axes (coinciding with areas of most recent volcanism) and the southern volcano. Thus the compositions of the magmas erupting on the two opposing ridges are indistinguishable magnetically. A relative magnetization minimum of 10–11 amp m⁻¹ occurs in the overlap basin. The magnetization may actually be lower there, and/or the magnetized portion of the oceanic crust may be considerably thinner.

data (Crane, 1987) and CYANA coverage to the south (Choukroune et al., 1984) indicate an increase in the axial fault density approaching the OSC. Such an increase would be expected with a decrease in the supply of melt since the likelihood of covering the faults and fissures would be less. The decrease in fault density may also reflect a decrease in the thickness of the thermal boundary layer associated with the cooling of oceanic crust (i.e. thinner crust and a lower magmatic budget).

Additional evidence for a diminishing magma supply towards the 12°54′ N OSC is the pattern of increasing fractionation toward the tip of the western spreading limb determined by Hekinian et al. (1985). Samples show an enrichment in titanium followed by a depletion in the forsterite content of the olivine approaching the tip. The southernmost samples contain phenocrysts of clinopyroxene whose composition is comparable to other fractionated low K tholeiites from the EPR (Hekinian et al., 1985). The occurrence of such a pattern of increasing fractionation suggests an increase in the channeling and/or distance from the source towards the tips of the OSC. Petrologic evidence that OSCs are generally boundaries between distinct source regions has been presented by Thompson et al. (1985) and Langmuir et al. (1986). They determined discrete magmatic provinces along the EPR in terms of both major elements and trace elements that are bounded by transform faults, OSCs or small changes in the strike of the axis (DevALs). Some OSCs even show distinct petrologic characters on opposing limbs, with one erupting enriched basalts and the other erupting highly fractionated compositions. From analyses of Ba/TiO_2 and Sr levels, Langmuir et al. (1986) observe a boundary at 12°54′ N between a segment erupting relatively enriched material and one erupting exclusively depleted MORB. While Hekinian et al. (1985) were unable to distinguish between a single or separate sources for the two ridges of the 12°54′ N OSC, they did determine a compositional diversity between the volcanics of the western spreading ridge and those of the basin and the eastern ridge.

Preliminary results from eight dredge hauls taken during our study show that the basalts are all moderately fractionated, typically depleted abyssal tholeiites. This area lacks ferrobasalts and there is no preferential concentration of more fractionated lavas on either limb of the OSC. On the western limb, the

five glass types have an average Mg number (Mg/ [$Mg + Fe^{+2}$]) of 0.615 ± 0.019; on the eastern limb 0.635 ± 0.026 (Natland et al., 1986). This is in contrast with the results from larger OSCs. For example, at 9° N ferrobasalts, andesites and dacites occur on the eastern limb, while ferrobasalts and alkali-enriched basalts occur on the other (Natland et al., 1986; Bender et al., 1986). Based on preliminary bulk-rock and trace-element analyses, Natland (unpublished data) finds that there are subtle distinctions between the east and west limbs of the OSC at 12°54′ N that suggest differences in source compositions and melting conditions beneath the two limbs, but the differences are small.

Similarly, the magnetic inversion performed from the Deep-Tow study at 12°54′ N indicates that the magnetization distribution is nearly the same for both the eastern and western spreading centers. There are no outstanding positive anomalies such as that detected over the 9°03′ N OSC which would indicate the presence of highly fractionated basalts. On the whole, the results of the magnetic inversion are inconclusive in relation to the existence of a single or separate sources for the two ridges of the small 12°54′ N OSC. Three possible scenarios arise from these results:

(1) The 12°54′ N OSC formed from two sources, but the magmas are so similar in composition that they are indistinguishable magnetically.

(2) The configuration formed from two sources, but these were connected at some time across the small offset, and a mixing of their magmas occurred (although Natland's (1986) preliminary geochemical analyses do not show any evidence for mixing).

(3) A two source model is not applicable to the 12°54′ N OSC and possibly many other short offset OSCs.

Of the three hypotheses, the first and second appear most probable in light of the evidence against a single throughgoing reservoir at the feature (Detrick et al., 1987; Langmuir et al., 1986). A continuous source model does not explain the indications for a decrease in the magma supply towards the tips on both limbs of the OSC, manifested in the increase in age of the volcanic flows, the increase in density of exposed faults and fissures, the disappearance of the axial graben and the increase in fractionation of the erupted basalts (Hekinian et al., 1985). A single throughgoing source is also inconsistent with the petrologic boundary at 12°54′ N determined by

Langmuir *et al.* (1986) which separates the eruption of relatively enriched petrologies from that of exclusively depleted MORB.

Unfortunately, available seismic data is equivocal. Results from a seismic refraction survey conducted 1 km south of the OSC (McClain *et al.*, 1985) suggest a single 4 km wide magma chamber, lending support to the second hypothesis involving coalescence of the separate sources. On the other hand, recent seismic reflection data (Detrick *et al.*, 1987) suggest that there is a short break in the north-south continuity of the axial magma chamber (<2 km) along the OSC. This break is so short, however, that the short-lived development of a connection between the spreading segments north and south of the OSC cannot be ruled out.

Lonsdale (1985) suggests that a reorganization of the Pacific-Cocos plate boundary approximately 3.5 Ma (Klitgord and Mammerickx, 1982) segmented the ridge forming a staircase of right-lateral offsets accommodated by OSCs. This implies that the offsets instigating formation of OSCs could persist for some time. As discussed earlier, there is strong evidence against the longevity of a single OSC, but the same evidence does not rule out repeated recurrence in the same location. Analysis of off-axis traces left by OSCs could provide insight as to whether these do recur and if so, whether they are stationary or migratory along the spreading ridge. Crane (1987) detected faulting within 7 km of the axis east of the 12°54′ N OSC (the same area as the off-axis ridge east of the eastern spreading center mentioned earlier) which is similar in width and orientation to the limbs of the present OSC. She suggests that this area is an abandoned ridge tip as predicted by our model for OSCs (Macdonald *et al.*, 1984). Recently collected SeaMARC II data do not reveal any significant off-axis scars further than 7 km from the rise. This observation rules out an origin earlier than approximately 0.1 my ago, and argues against the idea that this OSC is associated with the O'Gorman fracture zone as suggested by Schouten and Klitgord (1983).

As to the future of this OSC, it is not clear whether the western limb is propagating southward and will link up with the southern axis or vice-versa, but evidence is in favor of the former. Hekinian *et al.* (1985) suggest that the western limb is propagating southward on the basis of more recent volcanic activity on that spreading axis relative to the eastern ridge. Phipps Morgan and Parmentier (1985) have shown that gravity-spreading stresses associated with an anomalously shallow ridge may provide a sufficient driving force for the propagation of ridge tips, and relate the steepest along strike topographic gradient with the greatest propagation force. Such forces may be active here as well. The along axis bathymetric gradient of the northern segment (4.1 m km^{-1}) is somewhat steeper than that to the south (2.5 m km^{-1}), favoring a southward propagation of the western limb. It is also possible that the two spreading centers will not link. Macdonald *et al.* (in press) have suggested that an alternate mode of evolution for OSCs is 'self-decapitation', in which either spreading center may cut inside or outside of itself, repeatedly decapitating its own ridge tip. Crack propagation studies show that the crack propagation force drops significantly when the ratio of crack overlap to crack offset (L/W) exceeds 3. Applying this relation to spreading centers, they suggest that propagation of the individual spreading center tips may stall as (L/W) approaches 3, and here it is slightly greater than 3. If linkage has not yet occurred, then the next magmatic pulse which propagates along the ridge may be deflected away from the path of the existing ridge tip, decapitating the ridge tip in the process of 'self-decapitation'. Subsequent magmatic pulses may be deflected or 'derailed' from the existing path of the ridge because freezing of the axial magma chamber near ridge-axis discontinuities creates a core of coherent, unfaulted gabbroic rock along the spreading axis which is strong relative to the intensely faulted lithosphere on either side of the frozen magma chamber. In addition, the local stress field rotates near the discontinuity so that subsequent magma pulses and associated cracking fronts will tend to deflect away from the preexisting path of the ridge (Sempere and Macdonald, 1986a).

6. Summary

Our high resolution Deep-Tow survey near 12°54′ N yields numerous indications for a low magmatic budget in the vicinity of this small offset OSC. A high pillow to sheet flow ratio is observed, and no active hydrothermal vents were detected in the area which coincides with a low on the axial depth profile. The axial graben dies out approximately where a break in the axial magma chamber is inferred from multi-channel seismic results, and both the age and the degree of

fractionation of the lava flows increase towards the tips of the spreading axes. Greater distance from the magmatic source is also suggested by the increase in fault and fissure density approaching the offset. A 3-D magnetic inversion over the 12°54' N OSC produced no evidence for large variations in the magnetization of the source rocks. Possible explanations for this include a connection between the two original magmatic sources at some time in the past or a similarity in their magnetization and related composition.

Acknowledgements

References

Ballard, R. D., Hekinian, R., and Francheteau, J.: 1984, 'Geological Setting of Hydrothermal Activity at 12°50' N on the East Pacific Rise: A Submersible Study', Earth Planet. Sci. Lett. 69, 176–186.

Ballard, R. D., Holcomb, R. T., and van Andel, T. H.: 1979, 'The Galapagos Rift at 86° W, 3. Sheet Flows, Collapse Pits, and Lava Lakes of the Rift Valley', J. Geophys. Res. 84, 5407–5422.

Batiza, R. and Margolis, S. H.: 1986, 'A Model for the Origin of Small Non-overlapping Offsets (SNOOs) of the East Pacific Rise,' Nature 320, 439–441.

Bender, J., Langmuir, C. Natland, J., and Batiza, R.: 1986, 'Petrogenesis of East Pacific Rise High-silica Glasses,' EOS 67, 1254 (abs.).

Choukroune, P., Francheteau, J., and Hekinian, R.: 1984, 'Tectonics of the East Pacific Rise near 12°50' N: A Submersible Study', Earth Planet. Sci. Lett. 68, 115–127.

Crane, K.: 1987, 'Structural Evolution of the East Pacific Rise from 13°10' N to 10°35' N: Interpretations from SeaMARC I Data', Tectonophysics 136, 65–124.

Crane, K.: 1985, 'The Spacing of Rift Axis Highs: Dependence upon Diapiric Processes in the Underlying Asthenosphere?', Earth Planet Sci. Lett. 72, 405–414.

Crane, K.: 1979, 'The Galapagos Rift at 86°W: Morphological Waveforms; Evidence of a Propagating Rift', J. Geophys. Res. 84, 6011–6018.

Detrick, R., Buhl, P., Vera, E., Mutter, J., Orcutt, J., Madsen, J., and Brocher, T.: 1987, 'Multichannel Seismic Imaging of the Axial Magma Chamber Along the East Pacific Rise Between 9° N and 13° N', Nature 326, 35–41.

Fox, P. J. and Gallo, D. G.: 1984, 'A Tectonic Model of Ridge-Transform-Ridge Plate Boundaries: Implications for the Structure of Oceanic Lithosphere', Tectonophysics 104, 205–242.

Francheteau, J. and Ballard, R. D.: 1983, 'The East Pacific Rise near 21° N and 20° S: Inferences for Along-strike Variability of Axial Processes of the Mid-ocean Ridge', Earth Planet. Sci. Lett. 64, 93–116.

Hekinian, R., Auzende, J. M., Francheteau, J., Gente, P., Ryan, W. B. F., and Kappel, E. S.: 1985, 'Offset Spreading Centers near 12°53' N on the East Pacific Rise: Submersible Observations and Composition of the Volcanics', Mar. Geophys Res. 7, 330–359.

Hekinian, R., Fevrier, M., Avedik, F., Cambon, P., Charlou, J. L., Needham, H. D., Raillard, J., Boulegue, J., Merlivat, L., Moinet, A., Manganini, S., and Lange, J.: 1982, 'East Pacific Rise near 13° N: Geology of New Hydrothermal Fields', Science 219, 1321–1324.

Kennedy, S., Miller, S. P., Macdonald, K. C., and Tobler, W. R.: 1984, 'Improvements in the Accuracy of Gridding Geophysical Data', EOS 66, 115 (abs.).

Klitgord, K. D. and Mammerickx, J.: 1982, 'Northern East Pacific Rise: Magnetic Anomaly and Bathymetric Framework', J. Geophys. Res. 87, 6725–6750.

Langmuir, C. H., Bender, J. F., and Batiza, R.: 1986, 'Petrologic and Tectonic Segmentation of the East Pacific Rise', 5°30'–14°30' N, Nature 322, 422–429.

Lonsdale, P.: 1985, 'Non-transform Offsets of the Pacific-Cocos Plate and Their Traces on the Rise Flank', Geol. Soc. Am. Bull 96, 313–327.

Lonsdale, P.: 1983 'Overlapping Rift Zones at the 5.5°S Offset of the East Pacific Rise', J. Geophys. Res. 88, 9393–9406.

Macdonald, K. C., Sempere, J.-C., and Fox, P. J.: 1986, 'Reply: The Debate Concerning Overlapping Spreading Centers and Mid-ocean Ridge Processes', J. Geophys. Res. 91, 10501–10510.

Macdonald, K. C., Sempere, J.-C., and Fox, P. J.: 1984, 'The East Pacific Rise from Siqueiros to Orozco Fracture Zones: Along-strike Continuity of Axial Neovolcanic Zone and Structure and Evolution of Overlapping Spreading Centers', J. Geophys. Res. 89, 6049–6069.

Macdonald, K. C. and Fox, P. J.: 1983, 'Overlapping Spreading Centers: A New Kind of Accretion Geometry on the East Pacific Rise', Nature 302, 55–58.

Macdonald, K. C., and Fox, P. J.: 'The Axial Summit Graben and Cross-sectional Shape of the East Pacific Rise as Indicators of Axial Magma Chambers and Recent Volcanic Eruptions', Earth Planet. Sci. Lett. (submitted).

Macdonald, K. C., Sempere, J.-C., and Fox, P. J.: 'Tectonic Evolution of Ridge Axis Discontinuities by the Meeting, Linking or Self-decapitation of Neighboring Ridge Segments', Geology (in press).

Macdonald, K. C., Miller, S. P., Huestis, S. P., and Spiess, F. N.: 1980, 'Three-dimensional Modeling of a Magnetic Reversal Boundary from Inversion of Deep-tow Measurements', J. Geophys. Res. 85, 3670–3680.

McClain, J. S., Orcutt, J. A., and Burnett, M. S.: 1985, 'The East Pacific Rise in Cross-section: A Seismic Model', J. Geophys. Res. 90, 8627–8640.

Miller, S. P.: 1977, 'The Validity of the Geological Interpretation of Marine Magnetic Anomalies', Geophys. J. R. Astr. Soc. 50, 1–21.

Natland, J., Langmuir, C., Bender, J., Batiza, R., and Hopson, C.: 1986, 'Petrologic Systematics in the Vicinity of the 9° N Transform Offset, East Pacific Rise', EOS 67, 1254 (abs.).

Parker, R. L. and Huestis, S. P.: 1974, 'The Inversion of Magnetic Anomalies in the Presence of Topography', *J. Geophys. Res.* **79**, 1587–1593.

Parker, R. L.: 1972, 'The Rapid Calculation of Potential Anomalies', *Geophys. J. R. Astr. Soc.* **31**, 447–455.

Phipps Morgan, J. and Parmentier, E. M.: 1985, 'Causes and Rate Limiting Mechanisms of Ridge Propagation: A Fracture Mechanics Model', *J. Geophys. Res.* **90**, 8603–8613.

Schouten, H., Klitgord, K. D., and Dick, H. J. B.: 1987, 'Migration of Mid-ocean-ridge Volcanic Segments', *Nature* **303**, 835–839.

Schouten, H. and Klitgord, K. D.: 1983, 'Overlapping Spreading Centers on the East Pacific Rise', *Nature* **303**, 549–550.

Sempere, J.-C. and Macdonald, K. C.: 1986a, 'Overlapping Spreading Centers: Implications from Crack Growth Simulation by the Displacement Discontinuity Method', *Tectonics* **5**, 151–163.

Sempere, J.-C. and Macdonald, K. C.: 1986b, 'Deep-tow Studies of the Overlapping Spreading Centers near 9° N on the East Pacific Rise', *Tectonics* **5**, 881–900.

Sempere, J.-C., Macdonald, K. C., and Miller, S. P.: 1984, 'Overlapping Spreading Centers on the East Pacific Rise: A Three-dimensional Inversion of the Magnetic Field at 9°03′ N', *Geophys, J. R. Astr. Soc.* **79**, 799–811.

Spiess, F. N. and Lonsdale, P.: 1982, 'Deep-Tow Rise Crest Exploration Techniques', *Mar. Technol. Soc. J.* **16**, 67–75.

Spiess, F. N. and Tyce, R. C.: 1973, 'Marine Physical Laboratory Deep-Tow Instrumentation System', *SIO Ref.* 73–4.

Thompson, G., Ryan, W. B., Ballard, R. D., Hamuro, K., and Melson, W. G.: 1985, 'Axial Processes Along a Segment of the East Pacific Rise, 10°–12°', *Nature* **318**, 429–433.

Tobler, W. R.: 1979, 'Lattice Tuning', *Geographical Analysis* **11**, 36–43.

van Andel, T. H. and Ballard, R. D.: 1979, 'The Galapagos Rift Zone at 86° W, 2. Volcanism, Structure and Evolution of the Rift Valley', *J. Geophys. Res.* **84**, 5390–5406.

Vogt, P. R.: 1976, 'Plumes, Subaxial Pipe Flow and Topography Along the Mid-ocean Ridge', *Earth Planet. Sci. Lett.* **29**, 309–325.

Vogt, P. R. and Johnson, G. L.: 1975, 'Transform Faults and Longitudinal Flow Below the Mid-ocean Ridge', *J. Geophys. Res.* **80**, 1399–1428.